Pyrazolyl-Bridged Iridium Dimers. 17.[1] Tetrakis(alkene)diiridium(I) Complexes: $[Ir(\eta^2\text{-}C_2H_4)_2(\mu\text{-}Cl)]_2$ as a Precursor to $[Ir(\eta^2\text{-}C_2H_4)_2(\mu\text{-}pz)]_2$. Stereochemically Nonrigid Behavior of the Analogue $[Ir(\eta^2\text{-}C_2H_4)(\eta^2\text{-}C_2F_4)(\mu\text{-}Cl)]_2$

Michael A. Arthurs,† John Bickerton,† Stephen R. Stobart,* and Jihong (John) Wang

Department of Chemistry, University of Victoria, Victoria, British Columbia, Canada V8W 2Y2

Received July 1, 1997

The known bis(ethene) dimer $[Ir(\eta^2\text{-}C_2H_4)_2Cl]_2$, **1**, reacts with pyrazole in the presence of NEt_3 to form the deep purple pyrazolyl-bridged diiridium(I) analogue $[Ir(\eta^2\text{-}C_2H_4)_2(\mu\text{-}pz)]_2$ (**2**), which is however stable only in an atmosphere of ethylene gas. Reaction of **2** with MeI affords a pale orange product formulated as the $d^7{}_2$ diiridium(II) adduct $[Ir(Me)(\eta^2\text{-}C_2H_4)_2(\mu\text{-}pz)_2Ir(I)(\eta^2\text{-}C_2H_4)_2]$ (**3**) on the basis of its ^1H NMR spectrum, which provides no evidence for dissociation of **3** in solution (contrasting with the behavior of the corresponding adduct formed by the bis(cycloocta-1,5-diene) analogue of **2**); like **2**, **3** is unstable in the absence of excess ethylene. No congener of **2** could be obtained by similar treatment of the perfluoroethylene analogue $[Ir(\eta^2\text{-}C_2H_4)(\eta^2\text{-}C_2F_4)Cl]_2$ (**4**) of **1**, although **4** was found to be less unstable than previously suggested and has been fully characterized in solution below −70 °C by ^{19}F as well as ^1H NMR measurements. Thus, in acetone (but not in toluene or methylene chloride), **4** exists in equilibrium with two species, **4A** and **4B**, formulated as isomeric, mononuclear, 16e solvento complexes $[Ir(\eta^2\text{-}C_2H_4)(\eta^2\text{-}C_2F_4)Cl(S)]$, S = acetone; **4**:**4A**:**4B** (−90 °C) ca. 67:13:20. The slow-limiting ^{19}F NMR spectrum of **4**, which has been assigned with the aid of $^{19}F-^{19}F$ COSY data, unambiguously identifies a folded binuclear geometry that undergoes facile ring inversion of the chloro-bridged core, with $\Delta G_{200}^{\ddagger}$ ca. 39 kJ mol^{-1} estimated from the temperature-dependent NMR behavior. Coalescence data for signals attributed to mononuclear **4A** are consistent with "propeller rotation" of the C_2F_4 ligand at d^8 Ir(I), $\Delta G_{200}^{\ddagger}$ ca. 41 kJ mol^{-1}. Mononuclear, 18e, substituted cyclopentadienyl complexes $Ir(\eta^5\text{-}C_5H_4R)(\eta^2\text{-}C_2H_4)(\eta^2\text{-}L)$ (**5**, R = $COCO_2Et$, L = C_2H_4; **6**, R = COOMe, L = C_2F_4) can also be synthesized by bridge-cleavage reactions of **1** and **4**, respectively.

Introduction

We have a longstanding interest in the properties of diiridium complexes in which the two metal centers are connected through bridging pyrazolyl ligands.[2] The prototypal,[3] thermally stable, structurally characterized $d^8{}_2$ dimer $[Ir(COD)(\mu\text{-}pz)]_2$ (COD = η^4-cycloocta-1,5-diene; pzH = pyrazole) is specially significant in this context because it acts as a synthon for the bridged core framework: displacement of the terminal diolefin ligands by[4] CO and/or tertiary phosphines is facile, providing a simple route to a family of related diiridium(I) systems.[5] Addition of methyl iodide to the same COD dimer establishes equilibrium with its diiridium(II) adduct[6] $[Ir(Me)(COD)(\mu\text{-}pz)_2Ir(I)(COD)]$ (eq 1); however formation of the latter is only marginally favorable ($K \approx 10$), making this a system of special interest because kinetics of both forward and back reactions are accessible. We have suggested that the origin of such unusual behavior[7] may be restriction on Ir−Ir approach through repulsive interactions that develop between opposing endo methylene units[3] of the two COD carbocycles as they are brought toward one another along the Ir_2

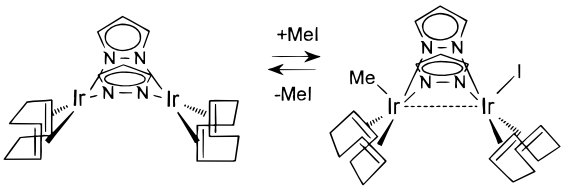

(1)

† Permanent address: Department of Chemistry and Environmental Sciences, Coventry University, Coventry, U.K. CV1 5FB.

(1) Part 16: Bushnell, G. W.; Fjeldsted, D. O. K.; Stobart, S. R.; Wang, J. *Organometallics* **1996**, *15*, 3785.

(2) Beveridge, K. A.; Bushnell, G. W.; Dixon, K. R.; Eadie, D. T.; Stobart, S. R.; Atwood, J. L.; Zaworotko, M. J. *J. Am. Chem. Soc.* **1982**, *104*, 920.

(3) Beveridge, K. A.; Bushnell, G. W.; Stobart, S. R.; Atwood, J. L.; Zaworotko, M. J. *Organometallics* **1983**, *2*, 1447.

(4) Harrison, D. G.; Stobart, S. R. *J. Chem. Soc., Chem. Commun.* **1986**, 285.

(5) Beveridge, K. A.; Bushnell, G. W.; Dixon, K. R.; Eadie, D. T.; Stobart, S. R.; Atwood, J. L.; Zaworotko, M. J. *Inorg. Chem.* **1984**, *23*, 4050.

(6) Coleman, A. W.; Eadie, D. T.; Stobart, S. R.; Zaworotko, M. J.; Atwood, J. L. *J. Am. Chem. Soc.* **1982**, *104*, 922.

(7) Brost, R. D.; Fjeldsted, D. O. K.; Stobart, S. R. *J. Chem. Soc., Chem. Commun.* **1989**, *8*, 488.

S0276-7333(97)00554-2 CCC: $15.00
Publication on Web 05/29/1998

vector. Since adverse steric influences of this type might be expected to be mitigated on replacement of the chelating COD diolefin by two independent monoolefin fragments, we decided to search for a route to a pyrazolyl-bridged bis(olefin)diiridium(I) analogue (of which rhodium congeners have been known for some time,[8] including one example[9] that was very recently characterized by X-ray crystallography).

Adopting as a logical precursor the chloro-bridged diiridium(I) complex[10] $[Ir(\eta^2\text{-}C_2H_4)_2Cl]_2$ (**1**), we found that bridge substitution of Cl by pz in dimer **1** can be used to synthesize its pyrazolyl analogue $[Ir(\eta^2\text{-}C_2H_4)_2(\mu\text{-pz})]_2$ (**2**) and that the latter reacts to completion with MeI, affording the adduct $[Ir(Me)(\eta^2\text{-}C_2H_4)_2(\mu\text{-pz})_2Ir(I)(\eta^2\text{-}C_2H_4)_2]$ (**3**), which shows no evidence (NMR) for dissociation in solution. Confirmation by X-ray crystallography of a contraction to within bonding range of the Ir_2 separation accompanying the **2**:**3** transformation was frustrated, however, because like some related compounds, including **1**, the products **2** and **3** are prone to loss of ethylene during manipulations carried out at ambient temperature. Parallel operations using the tetrafluoroethylene counterpart[11] $[Ir(\eta^2\text{-}C_2H_4)(\eta^2\text{-}C_2F_4)Cl]_2$ (**4**) of **1**, which were explored in an attempt to synthesize a less labile analogue of **2**, failed to yield such a product but instead focused our attention on the stereochemical properties of **4** itself, which is somewhat more stable thermally than has been suggested[11] previously.

We have found that the ^{19}F NMR spectrum of compound **4** is strongly temperature dependent: at −80 °C it becomes recognizable as the signature of a folded (vs planar) solution geometry for the bridged bimetallacyclic core framework, although only broad, featureless signals are observed under ambient conditions because of the fluxional character of the molecule. Reversible changes that occur between these extremes have been analyzed with the aid of COSY measurements that allow the low-temperature spectrum to be assigned unambiguously. We conclude that the coalescence behavior observed above −80 °C can be attributed to rapid ring inversion of the bridged binuclear unit, allowing the activation energy for this process to be estimated. Furthermore, while dimer **4** dissolves to only a very limited extent but is undissociated in either toluene or dichloromethane, in acetone-d_6 it exists as the major (∼70%) constituent in a dynamic equilibrium with two minor species that are formulated as the isomeric, planar, mononuclear solvento complexes $[Ir(\eta^2\text{-}C_2H_4)(\eta^2\text{-}C_2F_4)Cl(S)]$ (**4A**, **4B**). One of the latter also shows temperature-dependent ^{19}F NMR behavior, attributable to rapid exchange of fluorine environments that is consistent with propelloid rotation in solution of the π-bonded C_2F_4 group about the metal−fluoroolefin axis. This type of process was only recently characterized by Hughes et al.,[12] who showed that propeller rotation is not incompatible with a metallacyclopropane structure: facile C_2F_4 rotation (with an activation barrier as low as those found in some C_2H_4 analogues) was identified in both d^6 ML_5 and d^{10} ML_3 geometries. A brief report of some of the results discussed below was presented previously.[13]

Scheme 1

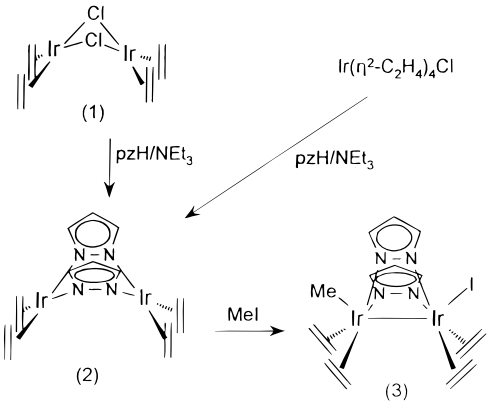

Results and Discussion

Pyrazolyl-Bridged Tetrakis(ethylene)diiridium Chemistry. Formation of the Methyl Iodide Adduct (3) of $[Ir(\eta^2\text{-}C_2H_4)_2(\mu\text{-pz})]_2$ (2). The deep red bis(ethylene)iridium(I) dimer $[Ir(\eta^2\text{-}C_2H_4)_2Cl]_2$ (**1**) was synthesized from the bis(cyclooctene) analogue through initial formation of the mononuclear tetrakis(ethylene) complex $Ir(\eta^2\text{-}C_2H_4)_4Cl$, as has been reported elsewhere.[10] Reaction of compound **1** with pyrazole at 0 °C in THF solution in the presence of excess NEt_3 resulted in a color change to deep purple, leading to recovery of the pyrazolyl-bridged dimer $[Ir(\eta^2\text{-}C_2H_4)_2(\mu\text{-pz})]_2$ (**2**) as a lustrous purple microcrystalline solid (Scheme 1). Treatment under an ethylene atmosphere of off-white[10] $Ir(\eta^2\text{-}C_2H_4)_4Cl$ with pyrazole and NEt_3 in THF at −50 °C afforded a gray product that is likely to be the η^1-pyrazolyl analogue $Ir(\eta^2\text{-}C_2H_4)_4pz$. While this gray material could be handled as a solid at room temperature, dissolution (NMR) or grinding (IR) led to formation of the characteristic purple color of **2**, and accordingly only the latter was detectable by mass spectrometry. Using methane chemical ionization, dimers **1** and **2** provided mass spectra that showed well-resolved molecular ions and fragmentation attributable to sequential stripping of C_2H_4. Compound **2** was further identified by microanalysis, by its ^1H NMR spectrum, which showed low-field resonances at δ 7.36 (d, 4H) and 6.05 (t, 2H) typical of μ-pz hydrogens and a well-resolved AA′XX′ pattern[10,14] centered on δ 2.69 (C_2H_4), and by a characteristic low-energy band (λ = 564 nm, ϵ 1.53 × 10^5) in the UV/visible spectrum.

Addition of methyl iodide to complex **2** in benzene solution resulted in discharge of the intense purple coloration and led to recovery of an orange-brown solid.

(8) Uson, R.; Oro, L. A.; Ciriano, M. A.; Pinillos, M. T.; Tiripicchio, A.; Tiripicchio Camellini, M. *J. Organomet. Chem.* **1981**, *205*, 247.
(9) Tejel, C.; Villoro, J. M.; Ciriano, M. A.; Lopez, J. A.; Eguizabal, E.; Lahoz, F. J.; Bakhmutov, V. I.; Oro, L. A. *Organometallics* **1996**, *15*, 2967.
(10) Onderdelinden, A. L.; van der Ent, A. *Inorg. Chim. Acta* **1972**, *6*, 420.
(11) van Gaal, H. L. M.; van der Ent, A. *Inorg. Chim. Acta* **1973**, *7*, 653.
(12) (a) Curnow, O. J.; Hughes, R. P.; Mairs, E. N.; Rheingold, A. L. *Organometallics* **1993**, *12*, 3102. (b) Hughes, R. P.; Tucker, D. S. *Organometallics* **1993**, *12*, 4736.
(13) Arthurs, M. A.; Bickerton, J.; Stobart, S. R.; Wang, J. *Abstracts of Papers*, XVIth International Conference on Organometallic Chemistry, Brighton, U.K., 1994.
(14) Cramer, R.; Kline, J. B.; Roberts, J. D. *J. Am. Chem. Soc.* **1969**, *91*, 2519. Guggenberger, L. J.; Cramer, R *J. Am. Chem. Soc.* **1972**, *94*, 3779. Cramer, R.; Mrowca, J. J. *Inorg. Chim. Acta* **1971**, *5*, 528. Cramer, R. *Inorg. Synth.* **1975**, *16*, 20.

Microanalytical data were consistent with adduct formation, and accordingly the ^{1}H NMR spectrum unequivocally identified the product **3** as that of two-center oxidative addition across the diiridium(I) center in **2**, to give a diiridium(II) complex (Scheme 1). Thus redissolution of the orange complex (CD_2Cl_2), which could be isolated in only low yield (17%) after purification, led to observation of an NMR spectrum in which three μ-pz proton environments are resolved (δ: 7.74, d; 7.36, d; 6.12, t) and equally populated, containing two independent AA′XX′ arrays (centered on δ 3.16, 2.86) and showing a singlet attributable to CH_3 protons (δ 2.59). Inequivalent H^{3,3a} and H^{5,5a} μ-pz hydrogens as well as inequivalent C_2H_4 multiplets confirm disubstitution that is unsymmetrical[1,5] along the Ir_2 axis, with chemical shift $\Delta\delta$ between the symmetrical wings of the AA′XX′ multiplets being 0.34 (around δ 3.16) and 0.68 ppm (around δ 2.86) compared with a related separation of 0.29 ppm for unoxidized **2**. The NMR data imply that there is rapid rotation about the Ir−ligand axis of the coordinated ethylene molecules at ambient temperature in both **2** and its methyl iodide adduct **3**, resembling behavior described recently[9] for the dirhodium(I) analogue [Rh(η^2-C_2H_4)$_2$(μ-pz)]$_2$ of **2**, although whether, like the latter, either **2** or **3** displays restricted alkene rotation at low temperature was not investigated owing to the limited stability in solution of these new products.

Neither free MeI nor unoxidized **2** was ever detected in NMR spectra of the purified adduct **3**: this, together with the conspicuous color change (from purple to orange), is consistent with (although does not prove) Ir−Ir bond formation accompanying oxidative addition {i.e., as has been established crystallographically for $d^7{}_2$ adducts derived from [Ir(CO)L(μ-pz)]$_2$ (L = PPh_3, CO)} and is in marked contrast with the behavior[6] of the unusual COD dimer[3] [Ir(COD)(μ-pz)]$_2$. Disappointingly, however, we were unable to obtain either **2** or **3** as crystals suitable for X-ray diffraction, so that although its properties suggest that product **3** is a further example of metal−metal-bonded[1−5] Ir(II)$_2$ (i.e., $d^7{}_2$), direct structural evidence remains unavailable. Complexes **2** and **3** deteriorated slowly as solids even in an atmosphere of ethylene and rapidly in solution; attempts to obtain further adducts analogous to **3** by reaction of **2** with diiodine or alkyl halides other than MeI were not successful.

Synthesis and Properties of the Chloro-Bridged (Ethylene)(tetrafluoroethylene)iridium(I) Dimer [Ir(η^2-C_2H_4)(η^2-C_2F_4)Cl]$_2$ (4). Reaction in pentane at −40 °C of the red chloro-bridged dimer **1** with tetrafluoroethylene was accompanied by a color change to pale yellow, as has been described.[11] In our hands the dimeric product, [Ir(η^2-C_2H_4)(η^2-C_2F_4)Cl]$_2$ (**4**), which had been only sketchily characterized previously,[11] proved to be sufficiently stable for microanalysis as well as mass spectrometry. Loss of both C_2H_4 and C_2F_4 was conspicuous in fragmentation of the molecular ion. NMR spectra were uninformative at ambient temperature, showing a single narrow proton resonance and two very broad signals in the ^{19}F range, but were strongly temperature-dependent: this is discussed in detail below. Treatment of complex **4** with pyrazole, in the manner used successfully to obtain the dimer **2**, led only to decomposition with no evidence for formation of any pyrazolyl-bridged product.

Scheme 2

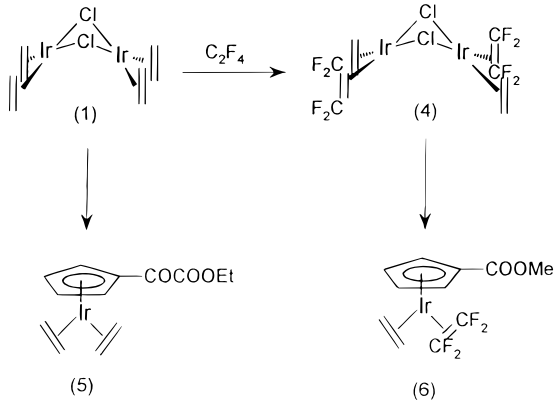

Both bis(olefin)iridium(I) dimers **1** and **4** proved to be susceptible to bridge cleavage, undergoing displacement of chloride by substituted cyclopentadienyl nucleophiles to give mononuclear cyclopentadienyliridium complexes **5** and **6** (Scheme 2). The two Ir(η^5-C_5H_4R)(η^2-C_2H_4)(η^2-L) species so obtained were respectively the ((ethoxycarbonyl)formyl)cyclopentadienyl (**5**, R = $COCO_2$Et, L = C_2H_4), which was expected to display a low barrier to ethylene rotation, and a (methoxycarbonyl)cyclopentadienyl (**6**, R = COOMe, L = C_2F_4), which is the first iridium analogue of the prototypal complex [Rh(η^5-C_5H_5)(η^2-C_2H_4)(η^2-C_2F_4)] (**7**) reported in 1969 by Cramer et al.[14]

Variable-Temperature NMR Spectra of the Bis(olefin)iridium(I) Dimers 1 and 4: Dynamic Stereochemistry of Compound 4. The structurally characterized Rh congeners[15] of compounds **1** and **4** are known to be of very limited solubility and have not been studied by NMR. The ^{1}H NMR spectrum of complex **1** has been recorded; at −55 °C ($CDCl_3$ solution), an AA′BB′ pattern (δ 2.7, 3.6) was observed that coalesced below 10 °C.[10] No data for the fluoroolefin analogue **4** are available.[11] We found that both **1** and **4** dissolved in acetone-d_6, which has a sufficiently low freezing point (−94 °C) to render it suitable for low-temperature NMR measurements. In this solvent, the ^{1}H NMR spectrum of dimer **1** showed at −70 °C only a single rather broad resonance, δ 3.82, that on warming broadened markedly and shifted upfield; from −20 °C the signal sharpened progressively, appearing at 21 °C as a broad line centered at δ 2.90. These data are not very informative but are consistent with rapid ethylene rotation as well as intermolecular exchange.[10]

Like that of its analogue **1**, the ^{1}H NMR spectrum of the tetrafluoroethylene dimer **4** (acetone-d_6 solution) consisted of a single line at ambient temperature, δ 3.72. On cooling, this signal collapses and then begins to resolve into three broad resonances centered at δ 3.9, 3.6, and 3.2. Below −20 °C, the central feature broadens rapidly while the outer two become somewhat sharper. No change is evident in the outer signals down to −80 °C, at which temperature the central signal is beginning to sharpen and resolve; no more definitive

(15) Dahl, L. F.; Martell, C.; Wampler, D. L. *J. Am. Chem. Soc.* **1961**, *83*, 1761. Ibers, J. A.; Snyder, R. G. *Acta Crystallogr.* **1962**, *15*, 923. Bonnet, J. J.; Jeannin, Y.; Kalck, P.; Maisonnat, A.; Poilblanc, R. *Inorg. Chem.* **1975**, *14*, 743.

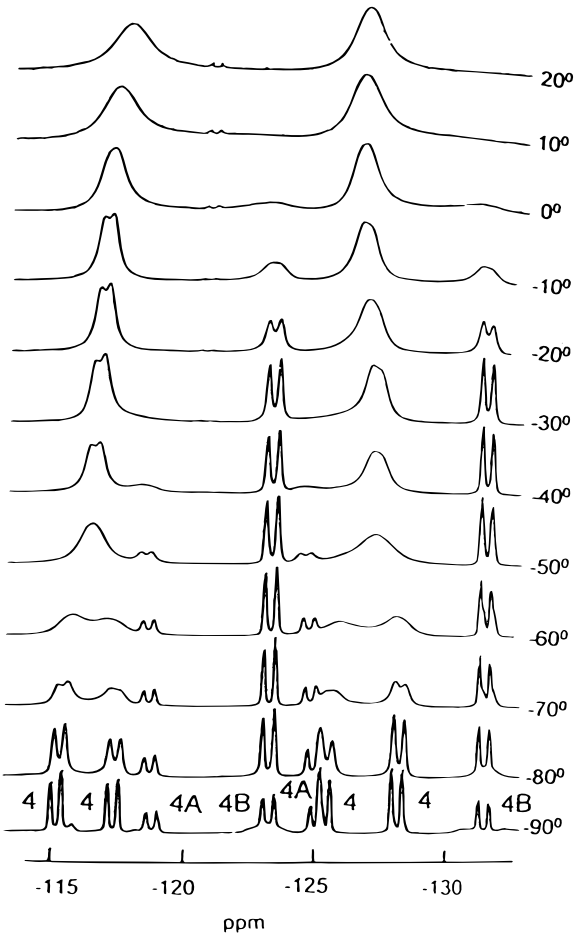

Figure 1. Variable-temperature ^{19}F NMR spectra (338.7 MHz; acetone-d_6) of $[Ir(\eta^2\text{-}C_2H_4)(\eta^2\text{-}C_2F_4)Cl]_2$ (**4**). Chemical shifts are upfield of $CFCl_3$.

Scheme 3

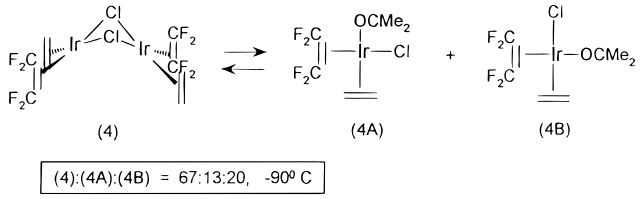

pattern emerges before all features broaden as the solution becomes glassy.

It is the appearance of the ^{19}F NMR spectrum of dimer **4** at ambient temperature that immediately identifies the unusual nature of this system. Figure 1 illustrates the dramatic and fully reversible changes that occur with varying temperature. As was reported earlier,[11] the complex is not very stable in solution and care is required to record reproducible data. At −90 °C, a well-resolved slow-limiting spectrum is reached: deconvolution of its rather complicated appearance is facilitated by differential collapse with increasing temperature of three independent constituent subspectra. The predominant set of signals is recognizable as a four-line AGMX pattern attributable to the diiridium(I) complex **4** (Scheme 3), and it is this array that loses definition first on warming. The two other sets of resonances consist of two-line coupled multiplets (AA′XX′), assigned to species **4A** and **4B** and labeled accordingly in Figure 1; one of these (**4A**) begins to

Chart 1

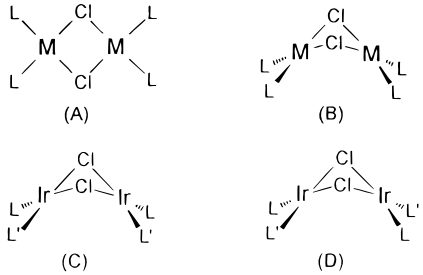

coalesce at only slightly higher temperature than does that of **4**, while the other (**4B**) shows no significant broadening below −20 °C. The equilibrium ratio **4**:**4A**:**4B** at −90 °C is 67:13:20. Because they were not detectable when either toluene-d_8 or CD_2Cl_2 was used as solvent in place of acetone, we suggest that **4A** and **4B** are mononuclear, square-planar, isomeric solvento species $[Ir(\eta^2\text{-}C_2H_4)(\eta^2\text{-}C_2F_4)Cl(S)]$ (S = acetone: Scheme 3), formed by bridge fragmentation and stabilized in equilibrium with **4** (Scheme 3) due to the donor character of the solvent. Further support for such a conclusion is provided by the observation of qualitatively similar changes with temperature in the ^{19}F NMR for the cyclooctene analogue $[Ir(\eta^2\text{-}C_8H_{14})(\eta^2\text{-}C_2F_4)Cl]_2$ of **4**, although this complex was found to exhibit poor solubility even in acetone.

Structural data for monoolefin complexes related to dimers **1**−**4** remain sparse for rhodium analogues and are nonexistent for iridium compounds. While it has been suggested on the basis of indifferent IR data that compounds **1** and **4** are planar,[10,11] **A** (Chart 1), X-ray crystal structures of $[RhL_2(\mu\text{-}Cl)]_2$ (L = CO, C_2H_4, $CH_2{=}CHCH{=}CMe_2$) reveal[15,16] folding across the Rh_2 axis, **B**, through angles that range from 116 to 123°, bringing the metal centers to within 3.09−3.17 Å of one another. These distances have been explained[17] using SCF−Xα−SW calculations in terms of a weak metal−metal interaction resulting from mixing of metal 4d(z^2) with a Rh−Cl bonding level; similar qualitative arguments based on a HOMO (Ir_2 σ^*) derived from 5d(z^2) overlap have been adopted to account for the ground-state structure, spectroscopy, and excited-state properties of diiridium complexes related to **2**. An unequivocal conclusion that may be drawn from the ^{19}F NMR data is that at low temperature in solution the dimer **4** possesses a folded structure **B**: observation of an AGMX pattern at the slow limit is consistent only with such an arrangement since the higher symmetry of the planar alternate **A** would generate an AA′XX′ spectrum, i.e. as is observed at −60 °C, Figure 1. While the NMR data do not distinguish between cis and trans ligand disposition across the Ir_2 axis (cis, **C**, C_s; trans, **D**, C_2), only one isomer is detected; and by analogy with related unsymmetrically substituted systems we suggest that this will be trans (**D**).

Progressive collapse of the resolved AGMX array assigned to **4** into a two-line spectrum at −60 °C (Figure 1) identifies the onset of a process that reduces the number of fluorine environments from 4 to only 2 on

(16) Coetzer, J.; Gafner, G. *Acta Crystallogr.* **1970**, *26B*, 985. Drew, M. G. B.; Nelson, S. M.; Sloan, M. *J. Chem. Soc., Dalton Trans.* **1973**, 1484.
(17) Norman, J. G.; Gmur, D. J. *J. Am. Chem. Soc.* **1977**, *99*, 1446.

the NMR time scale. Ring inversion of the bridged framework in the sense **B**:**A**:**B** will do this (exo vs endo and proximal vs distal discrimination, AGMX, reducing to only proximal vs distal, AA′XX′, i.e., averaging cis F environments): the barrier to such inversion is unknown but is estimated[16,17] to be low. Calculation[18] of the barrier for the site exchange from the coalescence temperature T_c (−55 °C) for **4** leads to a $\Delta G_c^{\ddagger}$ value of 38(1) kJ mol^{-1}. Propeller rotation of the C_2F_4 unit around the ligand−metal axis in the folded conformation **B** will however also effect F site averaging (into two pairs that occupy a trans relationship with one another) and could occur with[12] an activation barrier as low as this estimate. It is obvious that only one of these processes (i.e., ring inversion OR[9] propeller rotation) is being observed in the low-temperature regime (up to −60 °C): spectral simulation was recently used to identify[9] ethylene rotation (rather than ring inversion) as the single process responsible for similar averaging in the variable-temperature ^{1}H NMR spectrum of the rhodium(I) dimer [Rh(η^2-C_2H_4)$_2$(μ-pz)]$_2$, (i.e., the analogue of the new Ir complex **2**), but this conclusion is reached[19] on the basis of changes that are observed above (rather than below) the AA′XX′ coalescence temperature.

Distinction between ring inversion and propeller rotation as the mechanism responsible for the observed averaging in the dimer **4** therefore depends on identifying whether it is site exchange among cis or trans pairs of fluorine atoms that leads to coalescence. In the tetrafluoroethylene complexes investigated by Hughes et al., chemical shift differences are large between geminal fluorines (i.e., between proximal and distal sites) and smaller between cis fluorines; fluoroolefin propellor rotation averages pairs of nuclei that are trans to one another and are therefore well separated in the slow-limit spectrum.[12] By contrast, it is obvious that coalescence in the corresponding spectrum of **4** (Figure 1) occurs within high- and low-frequency halves of the limiting AGMX array, i.e. involving fluorines that experience a small chemical shift difference and may therefore be cis, consistent with ring inversion (not propeller rotation). This is a tenuous argument that has however been verified (vide infra) by use of ^{19}F−^{19}F COSY measurements to establish the gem and trans relationships in **4** conclusively. Spectral simulation with $^2J_{gem}$ 134.3, 140.4, $^3J_{trans}$ −24.4, −24.4, and $^3J_{cis}$ 5.0, 5.0 Hz gave good agreement with experimental data but generated line shapes that were identical for cis vs trans exchange profiles.

The ^{19}F−^{19}F COSY correlation map obtained for **4** at 188 K is shown in Figure 2, top. Strong cross-peaks identify those signals that are related by the largest couplings ($^2J_{gem}$ ca. 120 Hz) and are therefore due to geminal fluorines; similar relationships are also evident for the solvento species **4A** and **4B**. Geminal fluorines in **4** are interchanged by neither exchange mechanism (q.v.), and accordingly the COSY-related pairs are not those whose resonances coalesce with increasing temperature (see Figure 1). Changing the pre-FID delay to be optimal for a smaller coupling (ca. 30 Hz) generated the COSYL map shown in Figure 2, bottom, where accordingly the cross-peaks identify signals that are due to trans-disposed pairs of fluorine nuclei ($^3J_{trans}$ ca. 25 Hz); once again, these are not the pairs involved in the exchange, ruling out rotation as the mechanism for the latter. The resonances that coalesce with one another in the ^{19}F NMR spectrum may thus be assigned to cis pairs of fluorine nuclei, substantiating core ring inversion as the mechanism for site averaging.

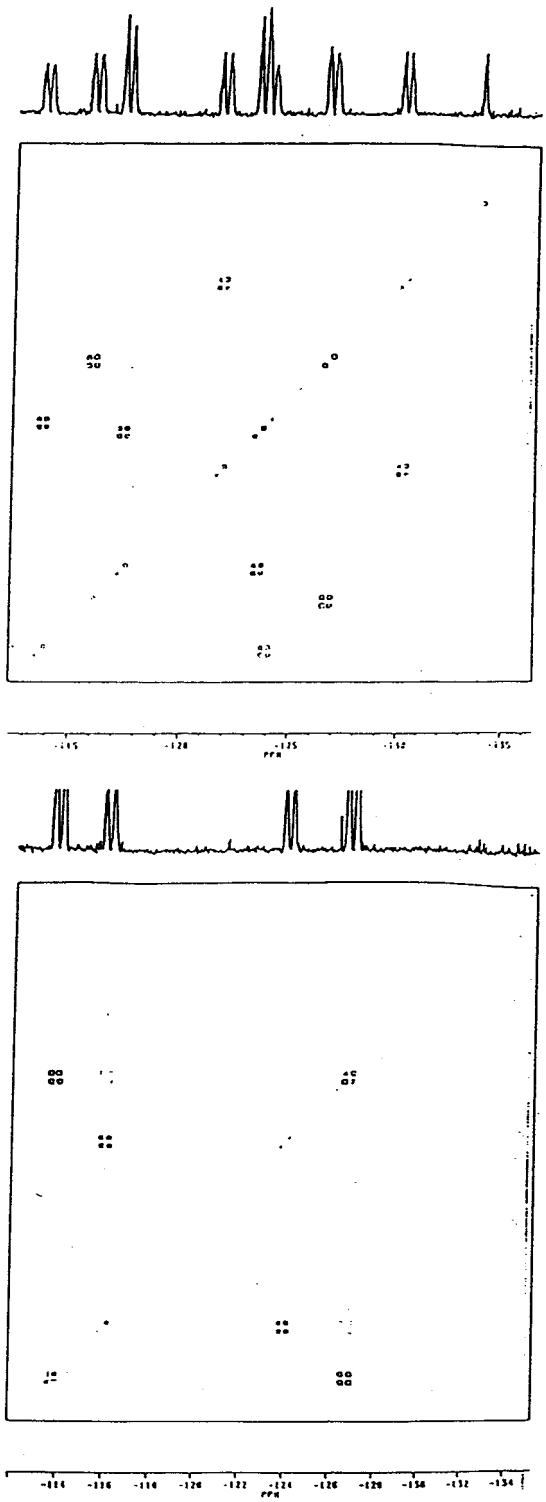

Figure 2. NMR correlation data for compound **4**: top, ^{19}F−^{19}F COSY map; bottom, COSYL map (i.e., with 0.01 s added to all τ values of standard 90°−τ−45° COSY).

(18) Szajek, L. P.; Lawson, R. J.; Shapley, J. R. *Organometallics* **1991**, *10*, 357.
(19) Oro, L. A.; Ciriano, M. A. Private communication.

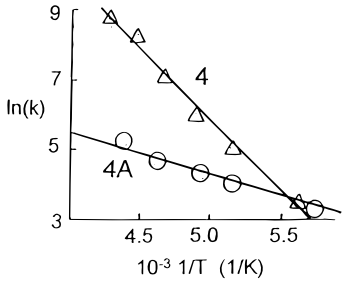

Figure 3. Arrhenius plots for the dynamic processes in **4** and **4A**.

Distinction between the two species tentatively identified as mononuclear, solvent-stabilized square d^8 configurations in Scheme 3 may be argued on the basis[20] of trans competition for electron density at Ir and acceptor capacity of Cl vs S. System **4A** shows an AA′XX′ pattern that progresses toward coalescence at ca. −50 °C (Figure 1); from T_c at −48 °C, a value of[18] $\Delta G_c^{\ddagger} = 41(2)$ kJ mol^{-1} may be estimated for what we suggest can only be a process in which mutually trans fluorine sites are exchanged by a rotational motion of the coordinated C_2F_4 about the olefin−metal axis, occurring trans to the electron-withdrawing Cl ligand. By contrast, the isomeric configuration **4B** reaches coalescence at a significantly higher temperature (ca. −11 °C, Figure 1): it is assigned a structure in which the donor S is trans to C_2F_4. It should be noted that in the low-temperature range there is no sign of any averaging of signals due to **4A** (or **4B**) with those assigned to **4** or of any resonances of the complexes with that of free C_2F_4 (−134 ppm).

The dynamic behavior displayed by **4** and **4A** was further investigated by using line-shape analysis to calculate exchange rates from[12,18] spectral simulation. Arrhenius treatment of the kinetics data led to reasonable straight-line plots that showed however a marked difference in slope for **4A** vs **4** (Figure 3), despite the comparable values for $\Delta G_c^{\ddagger}$. The source of this discrepancy was revealed by Eyring treatment of the data with least-squares analysis of plots[18] of $\ln(k/T)$ vs $1/T$ that were also approximately[21] linear in the low-temperature range. While values of $\Delta H^{\ddagger} = 32(2)$ kJ mol^{-1} and $\Delta S^{\ddagger} = -34(3)$ J K^{-1} (i.e., $\Delta G_{200}^{\ddagger} = 39$ kJ mol^{-1}) so derived for **4** are unremarkable, the much shallower slope of the Eyring plot for **4A** suggested a smaller enthalpy term and accordingly $\Delta H^{\ddagger} = 12(2)$ kJ mol^{-1}, with a very large $\Delta S^{\ddagger} = -147(3)$ J K^{-1} dominating a $\Delta G_{200}^{\ddagger} = 41$ kJ mol^{-1}. For each species, the ΔG datum agrees well with the cruder estimate based on coalescence temperature. If the rather surprising numbers for **4A** are real, they may be rationalized on the basis of its suggested structure, with C_2F_4 cis vs S (Scheme 3): exchange at the adjacent site of weakly bound acetone with the bulk could relieve steric restriction on alkene rotation (lowering $\Delta H^{\ddagger}$) and at the same time provide solvent organization consistent with a large, negative $\Delta S^{\ddagger}$.

The foregoing analysis of the ^{19}F NMR spectrum for **4**, **4A** and **4B** (Scheme 2) allows the temperature dependence observed in the ^{1}H NMR spectrum to be understood, although it cannot be interpreted in comparable detail. We suggest that, at −80 °C, the two outer resonances referred to earlier are due to **4** and **4B**, each with Cl trans to C_2H_4 and with the latter rotating rapidly, while the central feature that is broad and beginning to resolve is **4A**, with a higher barrier for rotation of C_2H_4 trans to the donor S (acetone). The single rather sharp resonance recorded at ambient temperature is attributable to rapid exchange among **4**, **4A**, and **4B** and possibly of ethylene among the latter.

Conclusions

The scope of the study described above was restricted by the discovery that replacement of the chelating diolefin ligands in the pyrazolyl-bridged diiridium prototype $[Ir(COD)(\mu\text{-pz})]_2$ by two independent terminal monoolefin units generates an analogue **2** that possesses quite limited stability. Thus the product $[Ir(\eta^2\text{-}C_2H_4)_2(\mu\text{-pz})]_2$ (**2**) could be manipulated satisfactorily only in an atmosphere of ethylene gas; and while it proved possible to isolate an adduct **3** with methyl iodide, the conduct of further related chemistry was judged to be impractical. The addition product **3** possesses all the characteristics of a metal−metal-bonded diiridium(II) (d^7_2) species, i.e. with Me in the exo (axial) site at one Ir center and I at the other, although such a structure has not been confirmed crystallographically. The behavior of **3** appears therefore to contrast with that of its COD analogue, which displays[3] an uncharacteristically long Ir_2 separation (3.112 Å, outside the range of Ir−Ir distances observed[2,4,5] in related d^7_2 adducts) and is extensively dissociated in solution.[6] We suggest that this comparison supports the proposition that the origin of the unusual properties of the COD dimer[3,6] is indeed inhibition of intermetallic approach through steric opposition exerted by the requirements of the two diolefin carbocycles. This effect is avoided in a related metal−metal bonded diiridium(II) perfluorobut-2-yne adduct (d^7_2: Ir−Ir = 2.623 Å) only by[5,23] severe buckling of the COD frameworks away from typical geometry. Although a bridge-substituted (μ-Me_2pz) dirhodium analogue of **2** was recently structurally characterized (nonbonding Rh_2 separation 3.096 Å: the shortest such approach yet observed[9]) and facile substitution of terminal ligands in the dirhodium congener[8] $[Rh(\eta^2\text{-}C_2H_4)_2(\mu\text{-pz})]_2$ of **2** has been shown to offer a useful synthetic strategy,[9] no binuclear rhodium(II) adducts that are analogues of **3** appear to have yet been prepared.[9] Our suggestion that the thermally unstable, gray compound isolated en route to dimer **2** is a mononuclear precursor $Ir(\eta^2\text{-}C_2H_4)_4$pz is supported by the recent characteriza-

(20) Arthurs, M.; Nelson, S. M.; Drew, M. G. B. *J. Chem. Soc., Dalton Trans.* **1977**, 779. Arthurs, M.; Nelson, S. M. *J. Coord. Chem.* **1983**, *13*, 29. Arthurs, M.; Al-Daffaee, H. K.; Haslop, J.; Kubal, G.; Pearson, M. D.; Thatcher, P. *J. Chem. Soc., Dalton Trans.* **1987**, 2615. Arthurs, M.; Piper, C.; Morton-Blake, D. A.; Drew, M. G. B. *J. Organomet. Chem.* **1992**, *429*, 257. Arthurs, M.; Bickerton, J. C.; Kirkley, M.; Palin, J.; Piper, C. *J. Organomet. Chem.* **1992**, *429*, 245. Arthurs, M.; Bickerton, J.; Kubal, G.; O'Sullivan, J.; Piper, C.; Hogarth, G.; Morton-Blake, D. A. *J. Organomet. Chem.* **1994**, *467*, 135. Hogarth, G.; Arthurs, M.; Bickerton, J. C.; Daly, L.; Piper, C.; Ralfe, D.; Morton-Blake, D. A. *J. Organomet. Chem.* **1994**, *467*, 145.

(21) Since linearity in both Arrhenius *and* Eyring plots is inherently inconsistent and because each of these approaches[22] pertains specifically to collision theory, neither may exactly describe the intramolecular exchange phenomena.

(22) Laidler, K. J. *Reaction Kinetics*; Pergamon: Oxford, U.K., 1963; Vol. 1.

(23) Bushnell, G. W.; Decker, M. J.; Eadie, D. T.; Stobart, S. R.; Vefghi, R.; Atwood, J. L.; Zaworotko, M. J. *Organometallics* **1985**, *4*, 2106.

tion[24] of a related complex $Ir(\eta^2\text{-}C_2H_4)_2(PEt_3)_2Cl$, as well as by the existence[10] of $Ir(\eta^2\text{-}C_2H_4)_4Cl$.

In what proved to be an unsuccessful attempt to expand the scope of chemistry related to the formation of **3** from **2**, bridge substitution of a tetrafluoroethylene precursor[11] $[Ir(\eta^2\text{-}C_2F_4)(\eta^2\text{-}C_2H_4)Cl]_2$ (**4**) was investigated. This led to the unexpected discovery that **4** is sufficiently stable for multinuclear NMR measurements, although unfortunately we were unable to isolate any pyrazolyl-bridged analogue. Thus the variable-temperature ^{19}F NMR spectrum of **4** yields convincing evidence for a folded geometry (**B**) at the slow limit of its dynamic range (−90 °C, acetone-d_6 solution), as well as for the existence of an equilibrium involving further species concluded to be solvent-stabilized isomeric mononuclear products (**4A**,**B**) of bridge fragmentation, while the COSY data identify the gem and trans fluorine pairs, confirming that the observed coalescence is the result of facile metallacyclic ring inversion ($\Delta G_{200}^{\ddagger}$ ca. 39 kJ mol^{-1}) that progressively averages the cis fluorine environments.

Coalescence of the multiplet pattern assigned to **4A** is interpreted as evidence for facile "propeller rotation" of the $\eta^2\text{-}C_2F_4$ ligand in a square d^8 configuration (Ir^I). The values obtained here for the barrier to such rotation ($\Delta G_{200}^{\ddagger} = 41$ kJ mol^{-1}) lie between those of 29 and 60 kJ mol^{-1}, respectively (which are presumably $\Delta G_c^{\ddagger}$ data although this was not specified), recently reported by Hughes et al.[12b] for the 16e complex $Ir(\eta^2\text{-}C_2F_4)(C_3Bu^t_3)(CO)$ vs its18e adduct $Ir(\eta^2\text{-}C_2F_4)(C_3Bu^t_3)(CO)(PPh_3)$; d^{10} (formally Ir^{-I}) character has been argued[12b] for each of these two species. It should be recalled that the Cramer complex, $[Rh(\eta^5\text{-}C_5H_5)(\eta^2\text{-}C_2H_4)(\eta^2\text{-}C_2F_4)]$ (**7**), shows[14] no evidence for $\eta^2\text{-}C_2F_4$ rotation up to 100 °C and that the iridium allyl $Ir(\eta^2\text{-}C_2F_4)(C_3H_5)(CO)(PPh_3)$ is[12] similarly rigid; these systems are both 18e d^8. Appropriate contextual analysis constructed around the theoretical conclusions of Hoffmann et al.[25] (who have emphasized the significance of steric effects) has already been offered by Hughes:[12] by comparison of the behavior of **4A** vs that of **7**, our data further implicate coordinative and/or electronic unsaturation as possible required conditions for facile "propeller rotation" of bound tetrafluoroethylene. The same sort of distinction is also evident for the cleavage products **5** and **6** of **4**: in these 18e, d^8 analogues of **7**, and where the $\eta^2\text{-}C_2F_4$ ligand in **6** is rigid on the NMR time scale, we observe substantial barriers to *ethylene* rotation ($\Delta G_c^{\ddagger}$ ca. 72 and 67 kJ mol^{-1}, repectively) that fit into the pattern[20] of related data. These barriers to C_2H_4 rotation are also close to those reported by Shapley and co-workers[18] for a family of further related 18e, d^8 Ir^I complexes and are clearly far higher than those for the 16e dimers **2** and **4**. Electron-deficient character of the latter vs 18e analogues will reduce the metallacyclic character of the olefin−metal interaction, and coordinative unsaturation is expected to act in a way that will enhance the orbital overlap required for facile olefin rotation.

(24) Aizenberg, M.; Milstein, D.; Tulip. T. H. *Organometallics* **1996**, *15*, 4093.
(25) Albright, T. A.; Hoffmann, R. A.; Thibeault, J. C.; Thorn, D. L. *J. Am. Chem. Soc.* **1979**, *101*, 3801.

Experimental Section

A. General Considerations. All manipulations were conducted under an atmosphere of argon using standard Schlenk techniques. Solvents for preparative application were dried and distilled using standard procedures. $IrCl_3{\cdot}xH_2O$ and $RhCl_3{\cdot}xH_2O$ (Johnson Matthey) and cyclooctene and pyrazole (Aldrich) were used as supplied. Gaseous C_2F_4 was bubbled directly from an old lecture-bottle container: there appears to be no remaining active commercial source of this material. Microanalyses were performed by Canadian Microanalytical Service Ltd. Mass spectra were measured on Kratos Concept-H and AEI MS-30 instruments. Mass spectral data for chloroiridium compounds refer to species containing $^{193}Ir^{35}Cl$ isotopes. The ^1H, ^{13}C, and ^{19}F NMR spectra were recorded on Bruker AC-250 and WM-360 spectrometers at 25 °C. Chemical shifts for ^{19}F were recorded as ppm upfield from $CFCl_3$ while ^1H and $^{13}C\{^1H\}$ shifts were measured as ppm downfield from tetramethylsilane. Temperature calibrations were performed with a capillary of ethylene glycol or methanol[26] as internal reference. NMR simulations and line-shape analyses were carried out using the DNMR5 program,[27] and $\Delta G_c^{\ddagger}$ values were calculated using the Eyring equation. Precursors including $[Ir(\eta^2\text{-}C_8H_{14})_2Cl]_2$, $[Rh(\eta^2\text{-}C_2H_4)_2Cl]_2$, and the sodium and thallium(I) cyclopentadienide derivatives were prepared by literature methods.[20]

B. Binuclear Iridium Compounds. (i) $[Ir(\eta^2\text{-}C_2H_4)_2Cl]_2$ (1). A pale orange suspension of $[Ir(\eta^2\text{-}C_8H_{14})_2Cl]_2$ (0.89 g, 1.0 mmol) in hexane (30 cm^3) was cooled to −50 °C and then stirred while a rapid stream of ethylene was bubbled in for 15 min. The gray precipitate of $[Ir(\eta^2\text{-}C_2H_4)_4Cl]$ was filtered out under ethylene and washed with three portions (3 × 10 cm^3) of pentane at −50 °C. Replacement of ethylene with an argon atmosphere and then warming to 0 °C gave deep red microcrystals (0.34 g, 0.6 mmol, 60%) of the product, **1**, which decomposed above 90 °C without melting. Attempted recrystallization resulted in decomposition. Anal. Calcd for $IrC_8H_{16}Cl_2$: C, 16.9; H, 2.8. Found:[28] C, 18.1; H, 2.9. MS (−CI/CH_4), *m*/*z*: 583 $(M + CH_5)^-$, 540 $(M - C_2H_4)^-$, 512 $(M - 2C_2H_4)^-$, 484 $(M - 3C_2H_4)^-$. ^1H NMR (acetone-d_6), δ: 2.90 (s, C_2H_4).

(ii) $[Ir(\eta^2\text{-}C_2H_4)_2(\mu\text{-pz})]_2$ (2). Addition of $[Ir(\eta^2\text{-}C_2H_4)_2Cl]_2$ (**1**; 0.57 g, 1.0 mmol) to a solution of pyrazole (0.14 g, 2.0 mmol) and triethylamine (0.6 cm^3, 4.2 mmol) in THF (25 cm^3) at 0 °C resulted in the development of a deep purple color. After 0.5 h, the solvent was removed and the residue was pumped to dryness (1 h, 10^{-2} mmHg). Extraction with THF (30 cm^3), filtration through neutral alumina (15 g), and concentration to 10 cm^3 volume was followed by dropwise addition of hexane (20 cm^3). Refrigeration (−28 °C, 24 h) gave purple microcrystals of the product (0.50 g, 0.79 mmol, 79%). Anal. Calcd for $Ir_2C_{14}H_{22}N_4$: C, 26.6; H, 3.5; N, 8.9. Found: C, 27.0; H, 3.7; N, 8.6. MS (+EI), *m*/*z*: 632 $(M)^+$; 604 $(M - C_2H_4)^+$; 576 $(M - 2C_2H_4)^+$; 548 $(M - 3C_2H_4)^+$. ^1H NMR (C_6D_6), δ: 7.36 (d, 4H, pz); 6.05 (t, 2H, pz, $J = 2.2$ Hz); 2.69 (m, 8H, C_2H_4). ^{13}C NMR (C_6D_6), δ: 135.07 (pz); 106.91 (pz); 50.14 (C_2H_4).

(iii) $[IrMe(\eta^2\text{-}C_2H_4)_2(\mu\text{-pz})_2IrI(\eta^2\text{-}C_2H_4)_2]$ (3). Pyrazole (0.043 g, 0.63 mmol) dissolved in a mixture of THF (1.0 cm^3) and NEt_3 (five drops) was added to a solution of $[Ir(\eta^2\text{-}C_8H_{14})_2Cl]_2$ (0.26 g, 0.30 mmol) in THF (15 cm^3). The mixture was stirred for 10 min, and then a rapid stream of ethylene was bubbled through the solution, resulting in a rapid change in color from red-brown to deep purple. Filtration under ethylene afforded a clear, inky purple solution. Evaporation of solvent

(26) Van Geet, A. L. *Anal. Chem.* **1970**, *42*, 679.
(27) Kleier, D. A.; Binsch, G. *J. Magn. Reson.* **1970**, *3*, 146; *QCPE* Program 165.
(28) Microanalytical data for **1** and **4** (each of which has[10,11] been reported previously, although owing to limited thermal stability neither was characterized by analysis or MS) lie outside acceptable ranges (except for Cl for **4**); however all MS and NMR data reported here are in full accord with the formulations proposed earlier.[10,11]

and pumping to dryness were followed by redissolution of the solid residue in dry benzene (10 cm^3). Addition of excess methyl iodide dissolved in benzene (10 cm^3) led to immediate discharge of the deep purple color, leaving an orange solution from which an orange-brown solid precipitated on addition of hexanes (20 cm^3). Redissolution in benzene, filtration, and then recovery by evaporation of solvent in a slow stream of ethylene afforded the orange product (0.04 g, 0.05 mmol, 17%). Anal. Calcd for $Ir_2C_{15}H_{25}IN_4$: C, 23.3; H, 3.3; N, 7.3. Found: C, 23.0; H, 3.1; N, 7.6. ^{1}H NMR (CD_2Cl_2), δ: 7.74 (d, 2H, J = 2.2 Hz, pz); 7.36 (d, 2H, pz); 6.12 (t, 2H, pz); 3.16 (m, 8H, C_2H_4); 2.86 (m, 8H, C_2H_4); 2.59 (s, 3H, Me).

(iv) [Ir(η^2-C_2F_4)(η^2-C_2H_4)Cl]$_2$ (4). Complex **1** (0.57 g, 1 mmol) was suspended in pentane (50 cm^3), and the suspension was stirred at −40 °C; then a rapid stream of tetrafluoroethylene was bubbled through the mixture for 20 min, during which the initial deep red color faded to pale yellow. The pale yellow precipitate so formed was filtered out under C_2F_4 at −20 °C, washed with cold pentane (3 × 20 cm^3), and then dried under a stream of argon. The yield of the product (0.45 g, 0.63 mmol) was 63%. Attempted purification by recrystallization led to decomposition. Anal. Calcd for $Ir_2C_8H_8F_8Cl_2$: C, 13.4; H, 1.1; Cl, 10.0. Found: C, 11.9; H, 1.1; Cl, 10.5. MS (+CI/CH_4), m/z: 712 $(M)^+$; 684 $(M - C_2H_4)^+$; 656 $(M - 2C_2H_4)^+$; 584 $(M - C_2H_4 - C_2F_4)^+$. ^{1}H NMR (acetone-d_6), δ: 3.71 (s). ^{19}F NMR (acetone-d_6, −90 °C) for **4**, δ: −115.20 (dd, F^1); −117.40 (dd, F^2); −125.37 (dd, F^3); −128.14 (dd, F^4). The COSY measurements discussed above establish that F^1, F^3 and F^2, F^4 are gem and F^1, F^4 and F^2, F^3 are trans (i.e. F^1, F^2 and F^3, F^4 are cis), while spectral simulation (DNMR5) with the following coupling constants matches the experimental spectrum: $J_{12} = J_{34} = 5.0$ Hz, $J_{14} = -24.3$ Hz, $J_{23} = -24.4$ Hz, $J_{13} = 140.4$ Hz, $J_{24} = 134.3$ Hz. ^{19}F NMR (aceteone-d_6 −90 °C) for **4A**, δ: −118.85 (dd, 2F); −125.00 (dd, 2F). ^{19}F NMR (acetone-d_6 −90 °C) for **4B**, δ: −123.35 (dd, 2F); −131.55 (dd, 2F).

C. Mononuclear Iridium(I) Complexes. (i) [Ir(η^5-$C_5H_4COCOOEt$)(η^2-C_2H_4)$_2$] (5). Sodium ((ethoxycarbonyl)-formyl)cyclopentadienide (0.38 g, 2.0 mmol) and **1** (0.57 g, 1.0 mmol) were stirred together in dry diethyl ether at ambient temperature for 12 h. The resulting suspension was filtered through Celite, the filtrate was evaporated, and then the residue was extracted with hexane (3 × 20 cm^3). The resulting solution was concentrated to 10 cm^3 volume, refrigeration of which (−5 °C, 24 h) gave white crystals of the product (0.25 g, 0.6 mmol), mp 98 °C. Anal. Calcd for $C_{13}H_{17}O_3Ir$: C, 37.75; H, 4.11. Found: C, 38.02; H, 4.24. MS, m/z: 414/412 $(M)^+$; 386, 384 $(M - C_2H_4)^+$; 358, 356 $(M - 2C_2H_4)^+$. ^{1}H NMR ($CDCl_3$), δ: 5.72 (t, $H^{3,4}$); 5.56 (t, $H^{2,5}$); 4.25 (q, CH_2); 1.96 (m, C_2H_4); 1.30 (t, CH_3). ^{13}C NMR ($CDCl_3$), δ: 174.72, 170.34 (CO); 91.18 (C^1); 90.08 ($C^{3,4}$); 83.59 ($C^{2,5}$); 60.92 (CH_2); 25.65 (C_2H_4); 16.05 (CH_3).

(ii) [Ir(η^5-$C_5H_4COOCH_3$)(η^2-C_2F_4)(η^2-C_2H_4)] (6). Solid [Tl(η^5-$C_5H_4COOCH_3$)] (33 g, 1.0 mmol) was added to a freshly prepared sample of dimer **4** (0.36 g, 0.5 mmol) dissolved in diethyl ether (30 cm^3), and then the mixture was stirred at 0 °C for 24 h. Evaporation of the solvent and extraction with hexane (3 × 20 cm^3), followed by filtration (Celite) and concentration of the filtrate, gave the product (0.22 g, 0.5 mmol) as a white powder. Anal. Calcd for $C_{11}H_{11}F_4O_2Ir$: C, 29.78; H, 2.48. Found: C, 29.42; H, 2.61. MS, m/z: 444, 442 $(M)^+$; 416, 414 $(M - C_2H_4)^+$; 316, 314 $(M - C_2H_4 - C_2F_4)^+$. ^{1}H NMR ($CDCl_3$), δ: 5.92 (t, $H^{3,4}$); 5.70 (t, $H^{2,5}$); 3.60 (s, CH_3); 2.72 (m, C_2H_4). ^{13}C NMR ($CDCl_3$), δ: 163.23 (CO); 93.71 (C^1); 90.67 ($C^{3,4}$); 89.19 ($C^{2,5}$); 85.92 (t, C_2F_4); 52.28 (CH_3); 33.07 (C_2H_4). ^{19}F NMR ($CDCl_3$), δ: −107.35 (m, 2F); −126.38 (m, 2F).

Acknowledgment. We applaud the skepticism of an anonymous reviewer who rejected chemical shift arguments as a sufficient basis for an assignment (which proved to be incorrect) of the ^{19}F NMR spectrum of complex **4** and suggested the COSY experiment; we are grateful to Drs. A. Clarke and O. Howarth, University of Warwick Centre for NMR, for carrying out the COSY measurements as well as for useful comments. We also thank the NSERC, Canada, for financial support, Dr. S. L. Grundy for preliminary experiments, Luis Oro and his group at the Universidad de Zaragoza for helpful discussions, and Johnson Matthey for a generous loan of iridium trichloride. M.A.A. thanks Coventry University, U.K., for a period of sabbatical leave.

Supporting Information Available: Arrhenius and Eyring plots for the dynamic behavior of **4** and **4A** and full size enlargements of both parts of Figure 2 (10 pages). Ordering information is given on any current masthead page.

OM970554J